

# Effects of Magnetic Field and Thermal Radiation on Flow and Heat Transfer Over a Radially Stretching Surface Subject to Variable Viscosity



Elsayed M. A. Elbashbeshy<sup>1\*</sup>, Hamada Galal Asker<sup>2</sup> and Khalid. M. Abdelgaber<sup>3</sup>

<sup>1</sup>Department of Mathematics, Faculty of Science, Ain Shams University, Abbassia, Cairo, Egypt

<sup>2</sup>Department of Physics & Engineering Mathematics, Faculty of Engineering, Ain Shams University, Cairo, Egypt

**Submission:** October 29, 2022; **Published:** January 06, 2023

**\*Corresponding author:** Elsayed M a Elbashbeshy, Department of Mathematics, Faculty of Science, Ain Shams University, Abbassia, Cairo, Egypt

## Abstract

The impact of variable viscosity, as a function of temperature, and thermal radiation on fluid boundary layers above a radially extending in the presence of magnetic field numerically investigated. The mathematical governing basic equations are solved by the numerical procedures like shooting and Runge–Kutta method. The influence of various values of the physical parameters on the velocity and temperature are analyzed. The skin friction and the Nusselt number are also calculated and examined.

**Keywords:** radially stretching surface, heat transfer, thermal radiation, magnetic field.

## Introduction

Flows via stretching surface occur in chemical compound technology, extrusion method, paper manufacturing, optical fiber production, plastic producing, rubber sheets production, and other fields. Sakiadis [1,2] pioneered the investigation of fluid boundary layer across a horizontal plate with constant speed. Elbashbeshy [3-9] probed the effects of injection/suction and thermal radiation on fluid boundary layers above steady/unsteady and exponentially stretching surfaces.

Velocity/thermal layers of different fluids above a radially expanding surface were analyzed by Ramly et al. [10], Soid et al. [11] and Butt et al. [12]. Makinde et al. [13] looked at the combined influence of thermal radiation, Brownian motion, MHD and changing viscosity on nanofluid boundary layer above a surface extended radically, whereas Mustafa et al. [14] looked at velocity profile of nanofluid above a surface expanded radically. In addition, Hayat et al. [15] investigated Jeffrey fluid across a surface expanded radically affected by certain physical properties.

All prior research was limited to fluids with invariant viscosity. This feature varies often with temperature. Elbashbeshy and Bazid [16] discussed the impact of viscosity, as a function of temperature,

on heat transmission across a mobile surface. Hossain et al. [17,18] investigated spontaneous convection flow across different surfaces for fluids with viscosity and thermal conductivity as functions of temperature. Molla and Hossain [19,20] probed natural convection streamline flow with viscousness and thermal conductivity as functions of temperature on a vertical wavy surface. Elbashbeshy [21] discussed the influence of viscosity, as a function of temperature, on fluid flow above a vertical plate under the impact of some parameters. Temperature-dependent viscousness on unsteady MHD fast decelerating flow through a wedge was explored by Ajay and Srinivasa [22]. The effect of changing viscosity on free convective fluid flow across a vertical plate was investigated by Elbashbeshy [23] in the presence of many conditions such as a magnetic field and radiation. The impact of viscosity, as a function of temperature, on boundary layer flow and heat transfer above a continuously moving vertical surface is presented by Ali [24].

The goal of this research is to look at how viscosity, as a function of temperature, and thermal radiation affect fluid velocity/thermal profiles over a radially expanding surface in the presence magnetic field.

**Mathematical formulation**

Affected by thermal radiation, two-dimensional, steady, and laminar boundary layer flow above a radially expanding surface investigated. As indicated in Figure 1, a coordinate system selection is made. The surface is stretched radially, along  $r -$  direction, with velocity  $U_w = ar$ , where  $a > 0$  is that the rate of stretching surface. The  $Z -$  direction is perpendicular to the  $r -$  direction. The surface is defined by  $z = 0$  and the flow are permitted only above it. A uniform transverse magnetic field of strength  $B_0$  is implemented in  $Z -$  direction, The magnetic Reynolds number is taken to be small enough so that the induced magnetic field can be neglected. The fluid is assumed to have constant physical characteristics, with the exception of fluid dynamic viscosity  $\mu[T]$ , which is supposed to be a function of fluid temperature  $T$  defined by [22]

$$\mu(T) = \frac{\mu_\infty}{1 + \gamma(T - T_\infty)} = \frac{\mu_\infty}{\gamma(T - T_\infty)}, T_e = T_\infty - \frac{1}{\gamma} \tag{1}$$

where  $\mu_\infty$  is the ambient viscosity of the fluid,  $\gamma$  is a thermal property of the fluid and  $T_\infty$  is the ambient temperature [16,23,24].

The dominant equations of the problem are:

$$\frac{\partial u}{\partial r} + \frac{u}{r} + \frac{\partial w}{\partial z} = 0 \tag{2}$$

$$u \frac{\partial u}{\partial r} + w \frac{\partial w}{\partial z} = \frac{1}{\rho_\infty} \left( \frac{\partial}{\partial z} (\mu \frac{\partial u}{\partial z}) \right) - \frac{\sigma B_0^2}{\rho_\infty} u, \tag{3}$$

$$u \frac{\partial T}{\partial r} + w \frac{\partial T}{\partial z} = \alpha \left( \frac{\partial^2 T}{\partial z^2} \right) - \frac{1}{\rho_\infty c_p} \frac{\partial q_r}{\partial z}, \tag{4}$$

where  $u(r, z)$  and  $w(r, z)$  represent fluid velocity components in the  $r -$  and  $Z -$  directions, respectively,  $\sigma$  is the electrical conductivity,  $\alpha$  is the thermal diffusivity of the fluid, and  $\rho_\infty$  is the fluid. The equations (2-4) are controlled by:

$$u(r, 0) = U_w, \quad w(r, 0) = 0, \quad T(r, 0) = T_w, \tag{5}$$

$$\lim_{z \rightarrow \infty} u(r, z) = 0, \quad \lim_{z \rightarrow \infty} w(r, z) = 0, \quad \lim_{z \rightarrow \infty} T(r, z) = T_\infty, \tag{6}$$

where  $U_w$  and  $T_w$  are the surface stretching linear velocity

and the surface constant temperature, respectively.

The radiation is approximated by

$$q_r = \frac{4\sigma^*}{3\lambda} \frac{\partial T^4}{\partial z}, \tag{7}$$

where  $\sigma^*$  is Stefan's constant and  $\lambda$  is the absorption coefficient. It is assumed that  $T^4$  is approximated linearly about  $T_\infty$  by neglecting the higher orders of its Taylor's series to get

$$T^4 = 4T_\infty^3 T - 3T_\infty^4. \tag{8}$$

Now, equation (4) becomes

$$u \frac{\partial T}{\partial r} + w \frac{\partial T}{\partial z} = \left( \alpha - \frac{16\sigma^* T_\infty^3}{3\rho_\infty c_p \lambda} \right) \frac{\partial^2 T}{\partial z^2} \tag{9}$$

Equation (2) is contented by a suitable choose of  $\psi(r, z)$  such that

$$u = -\frac{1}{r} \frac{\partial \psi}{\partial z}, \quad w = \frac{1}{r} \frac{\partial \psi}{\partial r}. \tag{10}$$

Introducing the similarity transformations

$$\eta = \frac{z}{r} \sqrt{R_e}, \quad \psi(r, z) = -\frac{r^2 U_w}{\sqrt{R_e}} f(\eta),$$

$$\theta(\eta) = \frac{T - T_\infty}{T_w - T_\infty} = \frac{T - T_e}{T_w - T_\infty} + \theta_e, \tag{11}$$

converts the partial differentia equations (3) and equation (9) into the ordinary ones:

$$f''' - \left(1 - \frac{\theta}{\theta_e}\right) (f')^2 + 2\left(1 - \frac{\theta}{\theta_e}\right) f f'' + \frac{1}{\theta_e - \theta} f'' \theta' - \xi f' = 0, \tag{12}$$

$$\theta'' + \frac{2Pr}{1 - R} f \theta' = 0, \tag{13}$$

where  $R_e = rU_w / \nu_\infty$  is Reynold number,  $\nu_\infty$  is the ambient kinematic viscosity of the fluid, the primes refer to the derivative of a function with respect to  $\eta$ ,  $\theta_e = (T_e - T_\infty) / (T_w - T_\infty)$  is the variable viscosity parameter,  $\xi = \sigma B_0^2 / \rho_\infty$  is the

magnetic parameter,  $Pr = \frac{\nu_\infty}{\alpha}$  is Prandtl number and

$R = 16\sigma^* T_\infty^3 / 3\alpha\rho_\infty c_p \lambda$  is thermal radiation parameter. Also, the similarity transformations, introduced in equation (11), turns the boundary conditions, given in equations (5-6), into the following form

$$f(0) = 0, \quad f'(0) = 1, \quad \theta(0) = 1, \quad \lim_{\eta \rightarrow \infty} f(\eta) = 0, \\ \lim_{\eta \rightarrow \infty} \theta(\eta) = 0, \quad (14)$$

The important practical quantities are the skin-friction coefficient,  $C_f$ , and the Nusselt number, Nu, defined by

$$C_f = \frac{2\tau_w}{\rho_\infty (U_w)^2}, \quad Nu = \frac{r(q_w + q_r)}{k(T_w - T_\infty)} \quad (15)$$

where  $\tau_w = (\mu \partial u / \partial z)_{z=0}$  is the shear tension on the surface and  $q_w = -k(\partial T / \partial z)_{z=0}$  is the heat flow at the surface. By using equation (11), the modified forms of quantities of equation (15) are

$$\sqrt{Re} C_f = \left( \frac{2\theta_e}{\theta_e - 1} \right) f''(0), \quad \frac{Nu}{\sqrt{Re}} = -(1 - R)\theta'(0). \quad (16)$$

### Numerical Procedure

The boundary value problem (12-14) is converted to an initial value one defined by:

$$\dot{x}_1 = x_2, \quad \dot{x}_2 = x_3, \\ \dot{x}_3 = \left( 1 - \frac{1}{\theta_e} x_4 \right) \left( (x_2)^2 - 2x_1 x_3 \right) + \frac{1}{\theta_e - x_4} x_3 x_5 - \xi x_2, \\ \dot{x}_4 = x_5, \quad \dot{x}_5 = -\frac{2Pr}{1-R} x_1 x_5 \quad (17) \\ x_1(0) = 0, \quad x_2(0) = 1, x_3(0) = s_1, \quad x_4(0) = 1, \\ x_5(0) = s_2, \quad (18)$$

where  $x_1 = f(\eta)$ ,  $x_4 = \theta(\eta)$  and the constants  $s_1$  and  $s_2$  are parameters that must be addressed during the solving

procedure.

$$X'(\eta) = F(\eta, X(\eta)), \quad 0 \leq \eta \leq \eta_{\max} \quad (19)$$

Where  $X(\eta) = [x_1(\eta) \quad x_2(\eta) \quad x_3(\eta) \quad x_4(\eta) \quad x_5(\eta)]$  and  $\eta_{\max}$  used as an adaptation for  $\eta \rightarrow \infty$ .

Two distinct orders,  $o$  and  $\hat{O} = o + 1$ , of Runge - Kutta formulae are considered. The procedure produces a set  $X_n$  approaching  $X(\eta_n)$  for  $0 = \eta_0 < \eta_1 < \dots < \eta_n = \eta_{\max}$ . Possible forms of  $X(\eta_{n+1})$  with orders  $o$  and  $\hat{O} = o + 1$  are

$$X_{n+1} = X_n + d_n \sum_{j=0}^S b_j M_j, \\ \hat{X}_{n+1} = X_n + d_n \sum_{j=0}^S \hat{b}_j M_j, \quad (20)$$

respectively, where  $\eta_{n+1} = \eta_n + d_n$ ,  $d_n$  is a step size to be adapted later to control the accuracy of approximation,  $S \geq 1$  is positive integer,

$$M_0 = F(\eta_n, X_n), \\ M_j = F\left(\eta_n + d_n \left( \sum_{k=0}^{j-1} a_{jk} \right), X_n + d_n \left( \sum_{k=0}^{j-1} a_{jk} M_k \right)\right), \quad (21)$$

And  $j = 1, 2, \dots, s$ . Using  $O = 4$  and  $S = 7$ , Bogacki and Shampine [25] describe how to evaluate the coefficients

$a_{jk}, b_j, \hat{b}_j \quad j = 1, 2, \dots, S$ , to yield the efficient set of formulae  $X_{n+1}$  (4th order) and  $\hat{X}_{n+1}$  (5th order).

The  $X(\eta_{\max}) = [X_1(\eta_{\max}) X_2(\eta_{\max}) X_3(\eta_{\max}) X_4(\eta_{\max}) X_5(\eta_{\max})]$  is created using the parameters  $S_1$  and  $S_2$ . Solving the equations  $x_1(\eta_{\max}) = x_4(\eta_{\max}) = 0$  yields the values for these parameters. The value of  $\eta_{\max}$  is gradually increased until the largest difference between any two consecutive values of  $S_1$  and  $S_2$  is less than the necessary accuracy  $\tau$ . The difference

between the two formulae  $X_{n+1}$  and  $\hat{X}_{n+1}$  is

$$e_{n+1} = \| X_{n+1} - \hat{X}_{n+1} \| . \tag{22}$$

Achieving the condition  $e_{n+1} \leq \tau$  makes the final approximation of  $X(\eta_{n+1})$  to be  $X_{n+1}$  or  $\hat{X}_{n+1}$ . If the condition is not satisfied, then  $e_{n+1}$  is utilized to adjust the step size  $d_n$  to be

$$\hat{d}_n = d_n \left( \frac{\tau}{e_{n+1}} \right)^{1/0} . \tag{23}$$

which is used to estimate the new values of  $X_{n+1}$  or  $\hat{X}_{n+1}$  till  $e_{n+1} \leq \tau$  is reached.

### Results and Discussions

On surface, the viscosity is defined by

$$\mu = \frac{\mu_\infty}{1 - \theta_e^{-1}} .$$

Obviously, when the value of  $|\theta|$  approaches infinity, the value of  $\mu$  approaches  $\mu_\infty$ . This demonstrates that as the value of  $|\theta|$  approaches infinity, the fluctuation of fluid viscosity is insignificant. Also, as the value of  $\theta_e$  approaches zero, the drift of fluid viscosity is clear. The viscosity parameter,  $\theta_e$ ,

cannot be settled between zero and one. For  $T_w - T_\infty > 0$ , the condition for gases is  $\theta_e > 1$ , whereas for liquids it is  $\theta_e < 0$ . For  $T_w - T_\infty > 0$ , the situation is reversed [16, 23, 24].

Figures 2 and 3 depict the fluctuations of skin friction coefficient,  $2\theta_e f''(0) / (\theta_e - 1)$ , and Nusselt number,  $-(1 - R)\theta'(0)$ , with regard to  $\theta_e$ . By raising  $\theta_e$ , the quantity  $2\theta_e f''(0) / (\theta_e - 1)$  rises while the quantity  $-(1 - R)\theta'(0)$  falls.

The impact of  $\theta_e$  on thermal profile is rendered in Figure 4. It has been found that when  $\theta_e$  grows, the thickness of the thermal boundary layer grows too. Recognize that a bigger  $\theta_e$  indicates a greater temperature gradient between the surface and the ambient fluid. As a result, convective heat transport accelerates.

The velocity profiles for various values of  $\theta_e$  are graphically displayed in Figure 5. Velocity distribution is reduced when the viscosity parameter is enhanced. Recognize that a grow in viscosity correlates to a grow in flow resistance, which suppress the fluid's velocity (Figure 2-7). The magnetic parameter,  $\zeta$ , is critical for managing fluid velocity/thermal layers in addition

to surface skin-friction/heat-flux. The values of  $\frac{2\theta_e f''(0)}{(\theta_e - 1)}$  and  $-(1 - R)\theta'(0)$  decrease as  $\zeta$  increases, as seen in Figures 6 and 7.

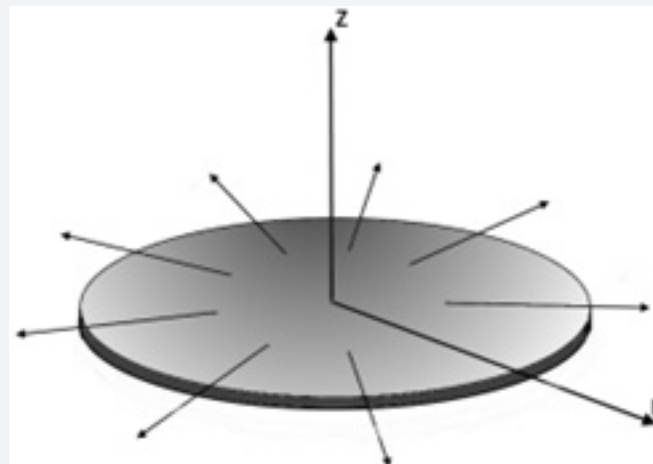


Figure 1: The problem schematic.

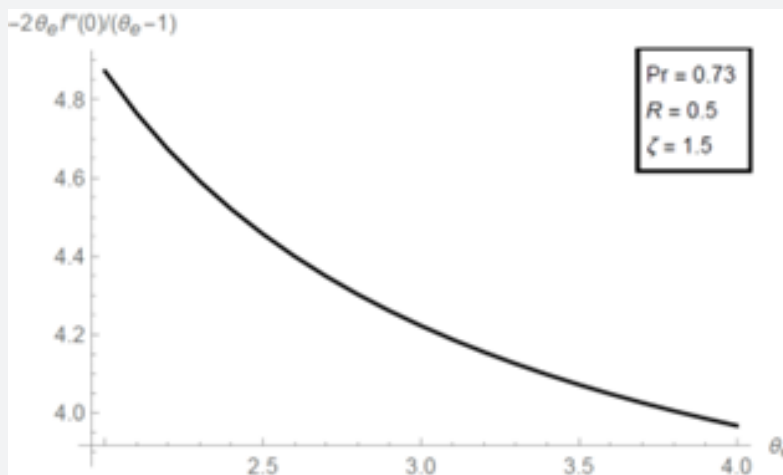


Figure 2: Negative impact of  $\theta_e$  on  $2\theta_e f''(0)/(\theta_e - 1)$  at  $Pr = 0.73, R = 0.5$  and  $\zeta$ .

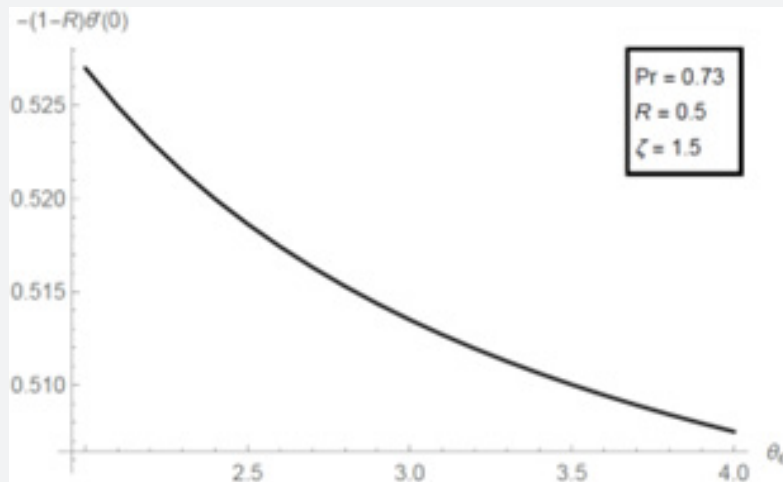


Figure 3: Impact of  $\theta_e$  on  $-(1-R)\theta'(0)$  at  $Pr = 0.73, R = 0.5$  and  $\zeta$ .

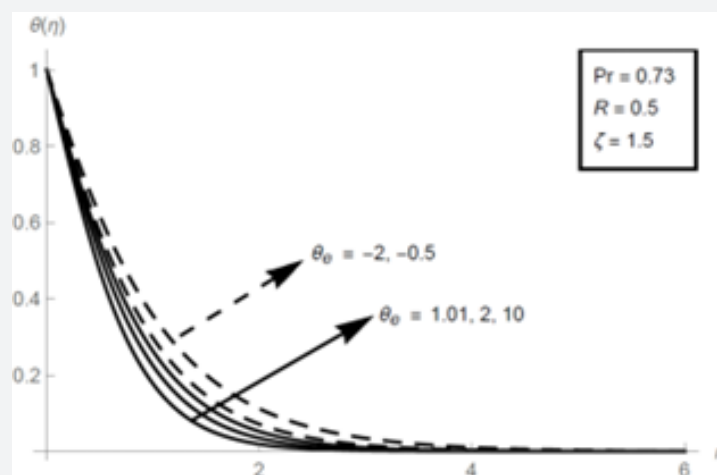


Figure 4: Impact of  $\theta_e$  on thermal profile at  $Pr = 0.73, R = 0.5$  and  $\zeta$ .

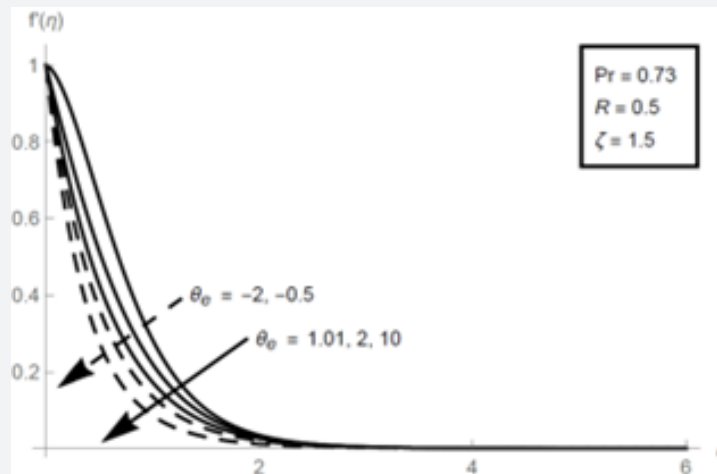


Figure 5: Impact of  $\theta_e$  on velocity profile atnd  $\zeta$  .

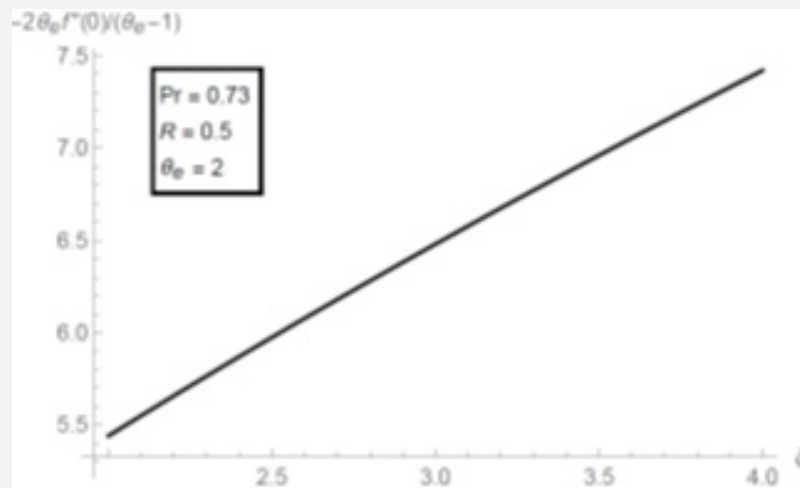


Figure 6: Negative impact of  $\zeta$  on  $2\theta_e f''(0)/(\theta_e - 1)$  atnd  $\theta_e$  .

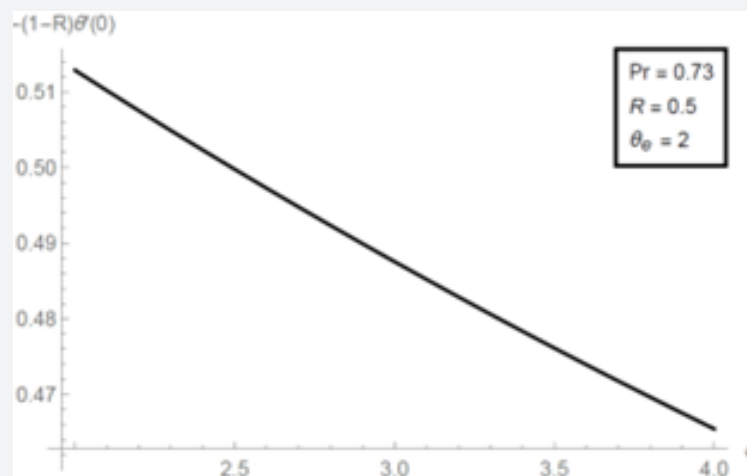


Figure 7: Impact of  $\zeta$  on  $-(1 - R)\theta'(0)$  at  $Pr = 0.73, R = 0.5$  and  $\theta_e$  .

As raising the values of  $\zeta$ , the fluid velocity boundary layers are reduced, as seen in Figure 8. On the other hand, enhancing the values of  $\zeta$  increases the thickness of the thermal boundary layer, as seen in Figure 9.

The Prandtl number is a dimensionless quantity that connects viscosity and thermal conductivity in a fluid. As a result, it assesses the link between the motion of a fluid and its heat

transfer capacity. As shown in Figures 10 and 11, increasing the Prandtl number,  $Pr$ , increases the values of  $2\theta_e f''(0) / (\theta_e - 1)$  and  $-(1 - R)\theta'(0)$ . Recognized that a higher Prandtl number fluid has a lower thermal conductivity (or a higher viscosity). For a larger value of  $Pr$ , the fluid thermal boundary layer will be thinner, as shown in Figure 12. and the surface heat flux will be higher, as shown in Figure 11.

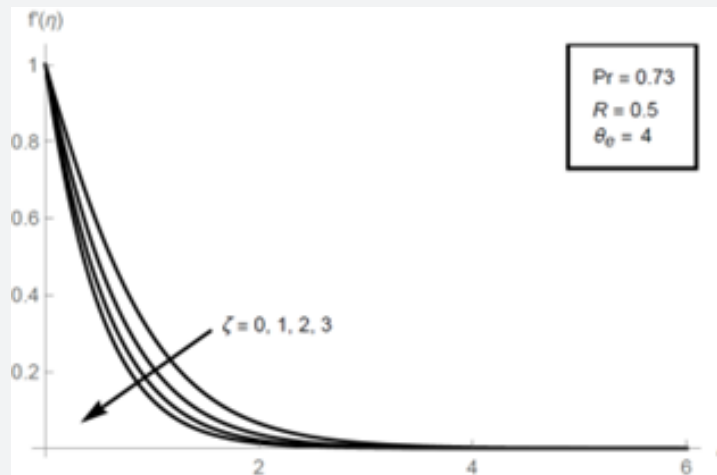


Figure 8: Impact of  $\zeta$  on velocity profile at  $Pr = 0.73, R = 0.5$  and  $\theta_e$ .

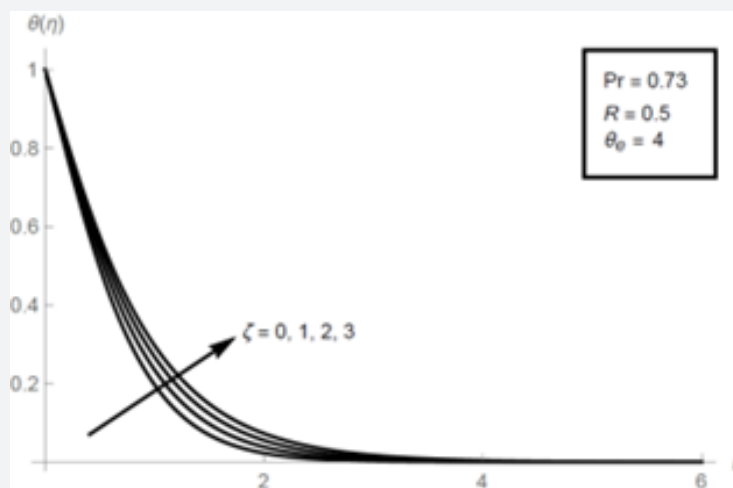


Figure 9: Impact of  $\zeta$  on thermal profile at  $Pr = 0.73, R = 0.5$  and  $\theta_e$ .

Given that raising the Prandtl number lowers the fluid temperature, which is inversely proportional to dimensionless

viscosity,  $\frac{\mu}{\mu_0}$ . As a result, a drop in fluid temperature causes a littler is in  $\mu_0$  dimensionless viscosity, and hence a small increase

in viscous forces that impede fluid motion. This explains why a grow in  $Pr$  causes the quantity  $2\theta_e f''(0) / (\theta_e - 1)$  to increase somewhat, see Figure 10, and the fluid velocity to drop slightly, as shown in Figure 13.

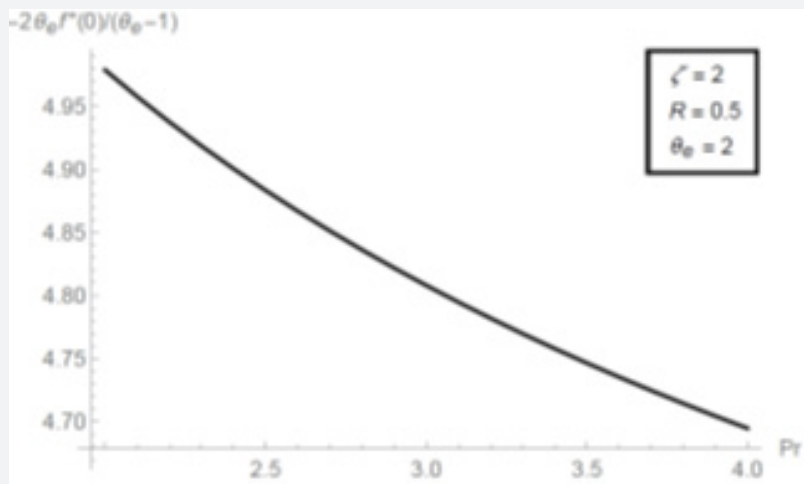


Figure 10: Negative impact of on at, and  $\zeta$ .

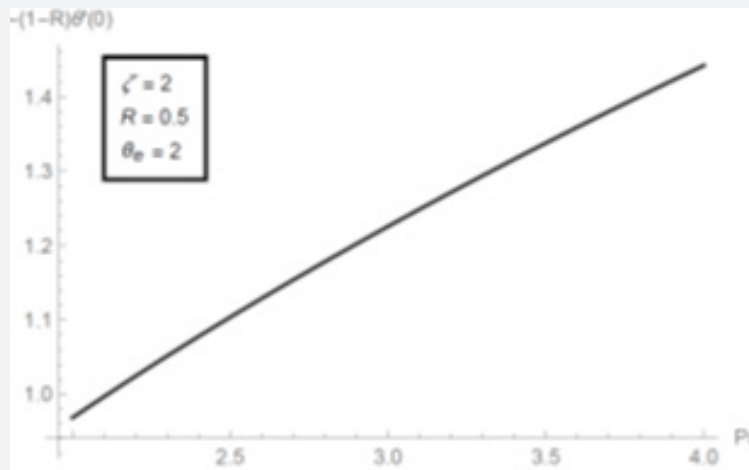


Figure 11: Impact of on at, and  $\zeta$ .

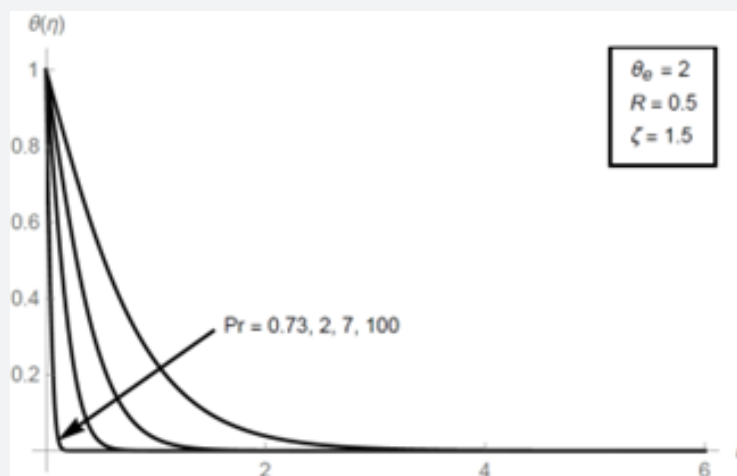


Figure 12: Impact of on thermal profile at  $\theta_e$ , and  $\zeta$ .



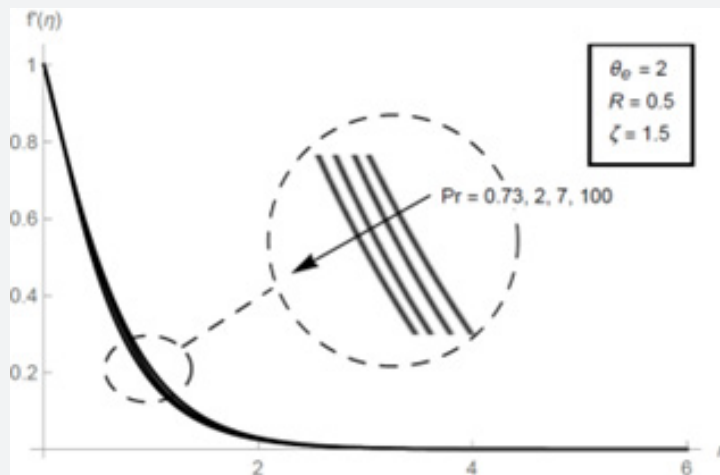


Figure 13: Slight impact of on velocity profile at  $\theta_0$ , and  $\zeta$ .

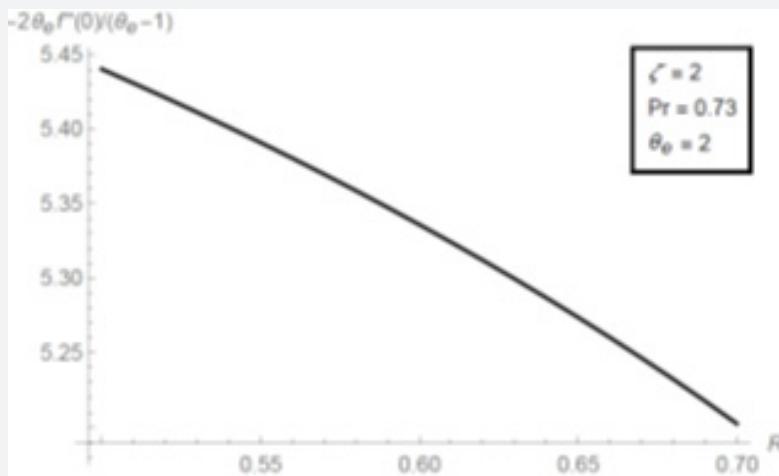


Figure 14: Negative impact of on at  $\theta_0$ , Pr and  $\zeta$ .

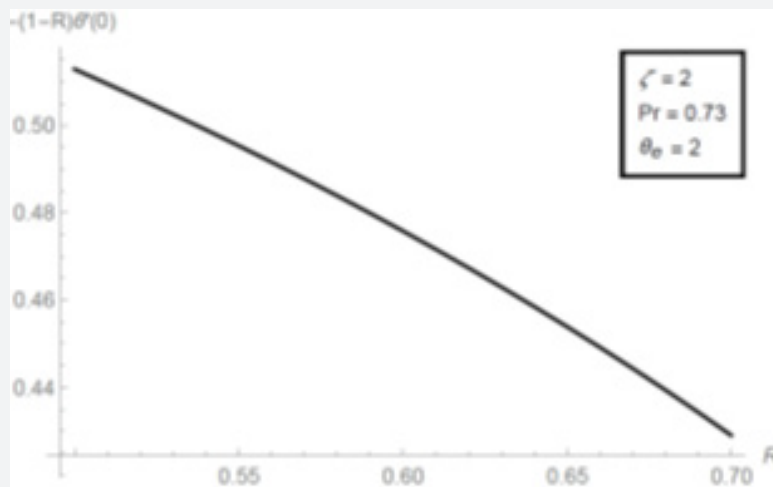


Figure 15: Impact of on at  $\theta_0$ , Pr and  $\zeta$ .

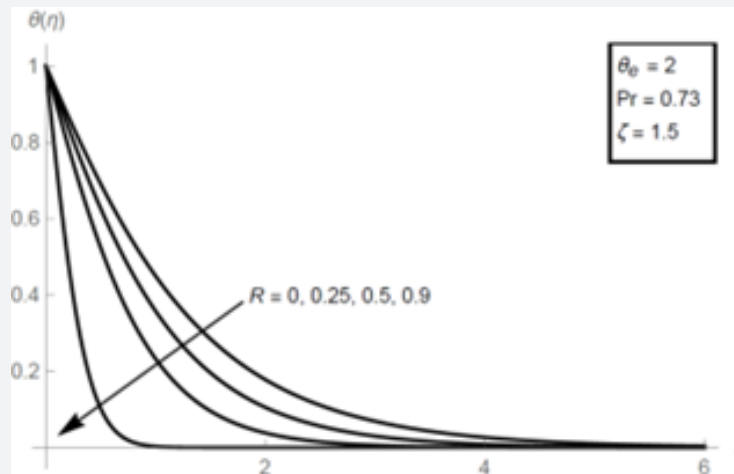


Figure 16: Impact of on thermal profile at  $\theta_e$ , Pr and  $\zeta$ .

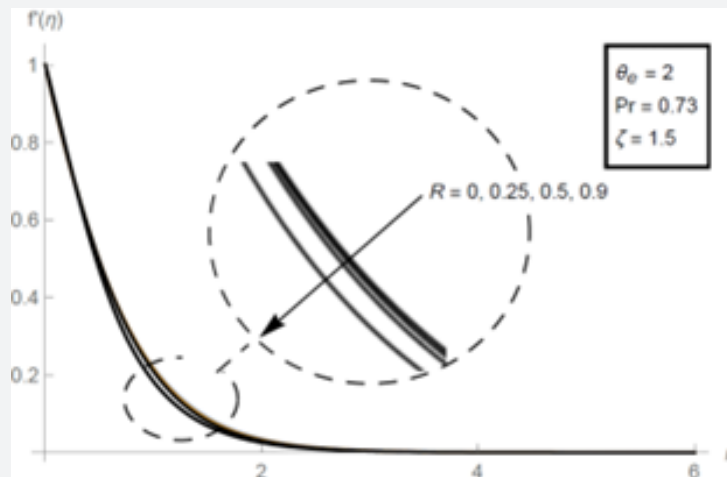


Figure 17: Slight impact of on velocity profile at  $\theta_e$  and  $\zeta$ .

The thermal radiation parameter, R, may be utilized to efficiently manage the thermal boundary layers. Figures 14 and 15 show that raising R causes the value of  $2\theta_e f''(0) / (\theta_e - 1)$  to increase and the value of  $-(1 - R)\theta'(0)$  to decrease.

As a result, increased thermal radiation lowers fluid temperature. Therefore, a drop in fluid temperature causes a little rise in dimensionless viscosity, and hence a small increase in viscous forces that impede fluid motion. This explains why an

increase in thermal radiation, R, causes the quantity  $\frac{2\theta_e f''(0)}{(\theta_e - 1)}$  to increase somewhat, see Figure 14, and the fluid velocity to drop slightly, as shown in Figure 17.

As seen in Figure 16, raising the thermal radiation parameter lowers the thermal boundary layer. These outcomes are consistent with predictions, because a reduction in  $\lambda$  is associated with a

grow in R. It is known that when  $\lambda$  falls, the rate  $\frac{\partial qr}{\partial r}$  increases, i.e., increasing the rate of radiative heat displaced from the fluid so the fluid temperature is lowered.

### Conclusion

The goal of this article is to use numerical modeling to examine the influence of viscosity, as a function of temperature, and thermal radiation on fluid velocity/thermal layers above a radially expanding surface in the presence magnetic field. The findings are visually displayed. It has been discovered that:

1. Variable viscosity and magnetic field reduce fluid velocity while raising fluid temperature.
2. The velocity and thermal profiles are reduced by growing Prandtl number or thermal radiation.
3. Surface shear stress is minimized by lowering viscosity, Prandtl number or thermal radiation and raising the magnetic value.

**Data availability** Data are available on request due to privacy or other restrictions.

### References

1. Sakiadis BC (1961) Boundary-layer behavior on continuous solid surfaces: I Boundary-layer equations for two-dimensional and axisymmetric flow, *AIChE Journal* 7(1): 26–28.
2. Sakiadis BC (1961) Boundary-layer behavior on continuous solid surfaces: II, The boundary layer on a continuous flat surface, *AIChE Journal* 7(2): 221–225.
3. Elbashbeshy EMA (1998) Heat transfer over a stretching surface with variable heat flux, *Journal of Physics D: Applied Physics* 31(16): 1951–1954.
4. Elbashbeshy EMA & M.A.A. Bazid (2004) Heat transfer over an unsteady stretching surface, *Heat Mass Transfer* 41(1): 14.
5. Elbashbeshy EMA & Emam TG (2011) Effects of thermal radiation and heat transfer over an unsteady stretching surface embedded in a porous medium in the presence of heat source or sink, *Thermal Science* 15(2): 477–485.
6. Elbashbeshy EMA (2001) Heat transfer over an exponentially stretching continuous surface with suction, *Archives of Mechanics* 53(6): 643–651.
7. Elbashbeshy EMA & M.A.A. Bazid (2003) Heat transfer over a stretching surface with internal heat generation. *Canadian Journal of Physics* 81(4): 699–703.
8. Elbashbeshy EMA & M.A.A. Bazid (2000) Effect of radiation on forced convection flow of a micropolar fluid over a horizontal plate, *Canadian Journal of Physics*, 78(10): 907–713.
9. Elbashbeshy EMA & Aldawody DA (2010) Effects of thermal radiation and magnetic field on unsteady mixed convection flow and heat transfer over a porous stretching surface. *International Journal of Nonlinear Science* 9(4): 448–454.
10. Ramly NA, Sivasankaran S & Noor NFM (2017) Zero and nonzero normal fluxes of thermal radiative boundary layer flow of nanofluid over a radially stretched surface. *Scientia Iranica* 24(6): 2895–2903.
11. Soid SK, Ishak A & Pop I (2018) Magnetohydrodynamic flow and heat transfer over a radially stretching/shrinking disk. *Chinese Journal of Physics* 56(1): 58–66.
12. Butt AS, Ali A, & Mehmood A (2017) Hydromagnetic stagnation point flow and heat transfer of particle suspended fluid towards a radially stretching sheet with heat generation. *Proceedings of the National Academy of Sciences India Section A: Physical Sciences* 87: 385–394.
13. Makinde OD, Mabood F, Khan W & Tshela M (2016) Magnetohydrodynamic flow of a variable viscosity nanofluid over a radially stretching convective surface with radiative heat. *Journal of Molecular Liquids* 219: 624–630.
14. Mustafa M, Hayat T & Alsaedi A (2012) Axisymmetric flow of a nanofluid over a radially stretching sheet with convective boundary conditions. *Current Nanoscience* 8(3): 328–334.
15. Hayat T, Waqas M, Shehzad SA & Alsaedi A (2015) Magnetohydrodynamic stagnation point flow of Jeffrey fluid by a radially stretching surface with viscous dissipation and joule heating. *Journal of Hydrology and Hydromechanics* 63(4): 311–317.
16. Elbashbeshy EMA & Bazid MAA (2000) The effect of temperature-dependent viscosity on heat transfer over a continuous moving surface. *Journal of Physics D Applied Physics* 33(21): 2716–2721.
17. Hossain A, Munir S & Rees DAS (2000) Flow of viscous incompressible fluid with temperature dependent viscosity and thermal conductivity past a permeable wedge with uniform surface heat flux. *International Journal of Thermal Sciences* 39(6): 635–644.
18. Hossain A, Munir S & Gorla R (2002) Combined convection from a vertical flat plate with temperature dependent viscosity and thermal conductivity. *International Journal of Fluid Mechanics Research* 29(6): 725–741.
19. Mamun M, Anwar H & Subba reddy G (2005) Natural convection flow from an isothermal horizontal circular cylinder with temperature dependent viscosity. *Heat and Mass Transfer* 41(7): 594–598.
20. Molla M & Gorla R (2009) Natural convection laminar flow with temperature dependent viscosity and thermal conductivity along a vertical wavy surface. *International Journal of Fluid Mechanics Research* 36(3): 272–288.
21. Elbashbeshy EMA & Ibrahim F (1993) Steady free convection flow with variable viscosity and thermal diffusivity along vertical plate. *Journal of Physics D Applied Physics* 26(12): 2137–2143, 1993.
22. Ajay CK & Srinivasa AH (2021) Temperature Dependent Viscosity Effects on Unsteady MHD Accelerating/Decelerating Flow Over a Wedge. *International Journal of Mathematics and Applied* 9(1): 19–126, 2021.
23. Elbashbeshy EMA (2000) Free convection flow with variable viscosity and thermal diffusivity along a vertical plate in the presence of the magnetic field. *International Journal of Engineering Science* 38(2): 207–213.
24. Ali M (2006) The effect of variable viscosity on mixed convection heat transfer along a vertical moving surface. *International Journal of Thermal Sciences* 45(1): 60–69.
25. Bogacki P and Shampine LF (1996) An efficient Runge-Kutta (4,5) pair. *Computers & Mathematics with Applications* 32: 15–28.



This work is licensed under Creative Commons Attribution 4.0 License

**Your next submission with Juniper Publishers  
will reach you the below assets**

- Quality Editorial service
- Swift Peer Review
- Reprints availability
- E-prints Service
- Manuscript Podcast for convenient understanding
- Global attainment for your research
- Manuscript accessibility in different formats

**( Pdf, E-pub, Full Text, Audio)**

- Unceasing customer service

**Track the below URL for one-step submission**

<https://juniperpublishers.com/online-submission.php>